

LET-99 determines spindle position and is asymmetrically enriched in response to PAR polarity cues in *C. elegans* embryos

Meng-Fu Bryan Tsou, Adam Hayashi, Leah R. DeBella, Garth McGrath* and Lesilee S. Rose†

Section of Molecular and Cellular Biology, University of California, Davis, CA 95616, USA

*Present address: Exelixis, South San Francisco, CA 94080, USA

†Author for correspondence (e-mail: lsrose@ucdavis.edu)

Accepted 1 July 2002

SUMMARY

Asymmetric cell division depends on coordinating the position of the mitotic spindle with the axis of cellular polarity. We provide evidence that LET-99 is a link between polarity cues and the downstream machinery that determines spindle positioning in *C. elegans* embryos. In *let-99* one-cell embryos, the nuclear-centrosome complex exhibits a hyperactive oscillation that is dynein dependent, instead of the normal anteriorly directed migration and rotation of the nuclear-centrosome complex. Furthermore, at anaphase in *let-99* embryos the spindle poles do not show the characteristic asymmetric movements typical of wild type animals. LET-99 is a DEP domain protein that is asymmetrically enriched in a band that encircles P lineage cells. The LET-99 localization pattern is dependent on PAR polarity cues and correlates with nuclear rotation and anaphase spindle pole movements in wild-type embryos, as

well as with changes in these movements in *par* mutant embryos. In particular, LET-99 is uniformly localized in one-cell *par-3* embryos at the time of nuclear rotation. Rotation fails in spherical *par-3* embryos in which the eggshell has been removed, but rotation occurs normally in spherical wild-type embryos. The latter results indicate that nuclear rotation in intact *par-3* embryos is dictated by the geometry of the oblong egg and are consistent with the model that the LET-99 band is important for rotation in wild-type embryos. Together, the data indicate that LET-99 acts downstream of PAR-3 and PAR-2 to determine spindle positioning, potentially through the asymmetric regulation of forces on the spindle.

Key words: Spindle orientation, Asymmetric division, Microtubules, Embryo, DEP domain, *C. elegans*

INTRODUCTION

In animal cells, the mitotic spindle determines the plane of cell division, thus affecting cell size, the position of daughter cells and the segregation of cytoplasmic determinants during the asymmetric division of polarized cells (Doe and Bowerman, 2001; Salmon, 1989). It is therefore of fundamental importance to understand how spindle positioning is regulated and how it is coordinated with cellular polarity. The *C. elegans* embryo is an ideal system in which to study mechanisms controlling spindle positioning, because wild-type embryos exhibit an invariant division pattern of both symmetrical and asymmetric divisions with characteristic nuclear and spindle positioning (Bowerman and Shelton, 1999; Gotta and Ahringer, 2001a; Rose and Kemphues, 1998b).

In *C. elegans*, the PAR proteins are required for cellular polarity and are asymmetrically localized at the cell periphery in response to the position of the sperm aster (Bowerman and Shelton, 1999; Goldstein and Hird, 1996; Rose and Kemphues, 1998b; Wallenfang and Seydoux, 2000). PAR-3, PAR-6 and PKC-3 are localized to the anterior periphery of the one-cell embryo, whereas PAR-2 is restricted to the posterior periphery. PAR-3/PAR-6/PKC-3 and PAR-2 are interdependent for localization and are required for the posterior localization of

PAR-1. PAR-1 is then necessary for the localization of MEX-5 and downstream cell fate determinants in anteroposterior (AP) domains (Bowerman and Shelton, 1999; Gotta and Ahringer, 2001a; Schubert et al., 2000). The first mitotic spindle is aligned along the anteroposterior axis, resulting in the differential segregation of cell-fate determinants upon division; cleavage is also unequal, generating a larger anterior AB cell and a smaller posterior P₁ cell. Anterior and posterior PAR domains are re-established in the P₁ cell, which also divides asymmetrically.

To produce the asymmetric cell division described above, several polarized nuclear and spindle movements are required, including nuclear centration, rotation and asymmetric spindle positioning (Bowerman and Shelton, 1999; Gotta and Ahringer, 2001b; Rose and Kemphues, 1998b). In the one-cell embryo, the female and male pronuclei meet in the posterior and then move to the middle of the embryo in a process called centration. As the pronuclei move, the entire nuclear-centrosome complex undergoes a 90° rotation so that the spindle will form on the AP axis. The spindle also moves and elongates asymmetrically towards the posterior during anaphase resulting in unequal cleavage. Similar polarized nuclear and spindle movements occur in the P₁ cell, which also undergoes asymmetric cell division. The nature of these

polarized movements suggests that they are mediated by asymmetric forces, at least some of which are generated by interactions between astral microtubules and the cell cortex/periphery, and are PAR dependent (Cheng et al., 1995; Grill et al., 2001; Hyman, 1989; Hyman and White, 1987; Keating and White, 1998; Waddle et al., 1994). However, the mechanisms by which the asymmetric localizations of the PAR proteins are transduced into asymmetric forces on the centrosomes and the spindle remain to be elucidated. One potential target of the polarity pathway is the microtubule motor cytoplasmic dynein. Inhibition of the function of dynein or its associated dynactin complex (to levels that still allow formation of a spindle) blocks nuclear centration and rotation in one-cell embryos (Gönczy et al., 1999). Some members of the dynein/dynactin complex appear enriched at the cell division remnant in two-cell embryos (Gönczy et al., 1999; Skop and White, 1998; Waddle et al., 1994) and could thus provide an asymmetric cue for rotation. However, because dynein appears uniformly localized at the cortex of one-cell embryos, its presence alone appears insufficient to explain the asymmetric nature of nuclear centration and rotation at this stage.

The PAR proteins could asymmetrically regulate dynein or other cortical proteins directly. Alternatively, there could be intermediate proteins that transduce the polarity cues to the spindle orientation machinery, analogous to the MEX-5 intermediate that connects PAR asymmetry with the localization of cell fate determinants (Bowerman and Shelton, 1999; Gotta and Ahringer, 2001a; Schubert et al., 2000). There are three criteria for such intermediates that function downstream of the PAR proteins in spindle positioning. First, mutations in an intermediate gene should affect spindle position but not asymmetric localization of PAR proteins and other aspects of polarity. Second, an intermediate protein should directly or indirectly regulate the generation of forces on the spindle, and thus mutants should exhibit failures in some or all of the polarized nuclear and spindle movements described above. Third, at least one component of an intermediate pathway should be asymmetrically activated or localized in response to the PAR proteins.

Several genes have been described that fit the first two criteria for an intermediate. These include the trimeric G-protein subunit encoding genes *gpb-1* (G protein β -1), *gpc-2* (G protein γ -2), *goa-1* (G protein α -1, class O) and *gpa-16* (G protein α -16), as well as *ric-8* (Gotta and Ahringer, 2001b; Miller and Rand, 2000; Zwaal et al., 1996). Comparisons of the phenotypes of embryos depleted for GOA-1, GPA-16 and GPB-1 singly and in combinations suggest that the G α s function redundantly in asymmetric positioning of the first spindle, while G $\beta\gamma$ functions in centrosome migration and nuclear rotation (Gotta and Ahringer, 2001b). RIC-8 appears to play a positive role in GOA-1 signaling in the embryo (Miller and Rand, 2000). The G proteins are uniformly localized to the cortex and to microtubule asters and thus are not likely to depend on the PAR pathway for localization, but could be asymmetrically activated by the PARs.

Previous work on the *let-99* gene shows that it also fits the first two criteria for an intermediate gene (Rose and Kemphues, 1998a). Recessive maternal effect lethal mutations in *let-99* cause defects in nuclear rotation in the P lineage, while spindles in the AB lineage sometimes align ectopically on the

anteroposterior axis; the localizations of PAR proteins and other polarity markers are normal. In addition, nuclear centration in one-cell mutant embryos is incomplete and the nuclear-centrosome complex exhibits a 'nuclear rocking' phenotype. These phenotypes overlap with those of G-protein-depleted embryos (Gotta and Ahringer, 2001b; Rose and Kemphues, 1998a; Zwaal et al., 1996) (Tsou and Rose, unpublished). Thus, the *let-99* gene plays a crucial role in specifying spindle orientation after polarity is established, potentially as part of the G-protein signaling pathway.

We provide further data that *let-99* is required for asymmetric forces on nuclei and spindles and new evidence that LET-99 fits the third criteria for an intermediate protein in the PAR pathway. The nuclear rocking exhibited by *let-99* embryos is a hyperactive dynein-dependent movement and anaphase spindle pole movements are also abnormal, suggesting a role for LET-99 in regulating force generation. LET-99 is a novel DEP-domain containing protein that is enriched in a unique asymmetric pattern at the periphery of P cells in response to PAR polarity cues. These results indicate that LET-99 functions as an intermediate that transduces polarity information to the machinery that positions the mitotic spindle.

MATERIALS AND METHODS

Strains and maintenance

C. elegans were cultured using standard conditions (Brenner, 1974). The following strains were used in this study:

N2, wild type Bristol;

KK705, *let-99(it141) unc-22(e66)/nT1 [unc(n754) let]*;

KK805, *let-99(s1201) unc-22(s7)/nT1 [unc(n754) let]*;

RL19, *let-99(or81) unc-22(e66)/nT1*;

CB3843, *fem-3(e1996)/dpy-20(e1282) unc-24(e138)*;

KK302, *unc-22(e66) dpy-4(e1166)*;

NG2198, *dpy-20(1282) ham-1(n1438) unc-31(e169)*;

KK747, *par-2(lw32) unc-45(e286ts)/sC1 [dpy-1(e1) let]*; and

KK653, *par-3(it71) unc-32(e189)/qC1*.

Double mutants were as described previously (Rose and Kemphues, 1998a). Strains were provided by the *C. elegans* Genetics Center [N2, CB3843; the Garriga laboratory (NG2198), the Kemphues laboratory (KK strains)] or constructed during this study. The *or81* allele used to construct RL19 was kindly provided by B. Bowerman (University of Oregon). All worms were grown at 20°C; filming was at 23–25°C. N2 was used for all wild-type controls.

Cloning and RNA analysis

The *let-99* gene was mapped to the *ham-1 unc-31* region using standard meiotic recombination; details are in Wormbase (Stein et al., 2001). Cosmids (from the *C. elegans* Sequence Consortium) and subfragments were co-injected with the pRF4 plasmid containing the dominant visible marker *rol-6(e187)* (Mello and Fire, 1995), into KK705 hermaphrodites. Heritable Roller lines were obtained and Roller *let-99* segregants that gave rise to more than five adult progeny were scored as rescued. For mutant alleles, genomic DNA from *let-99* hermaphrodites was amplified using Taq polymerase and primers flanking the *let-99*-coding region; PCR products were cloned into pGEMT Easy and three independent PCR reaction products were sequenced for each allele.

cDNAs were isolated from *C. elegans* libraries (gifts from B. Barstead and P. Okkema) and RNA isolation, northern blotting and hybridization were performed (see Watts et al., 2000). To determine the 5' end of the *let-99* transcript, first strand cDNA was synthesized using a *let-99*-specific primer and polyA⁺ mRNA, then amplified with

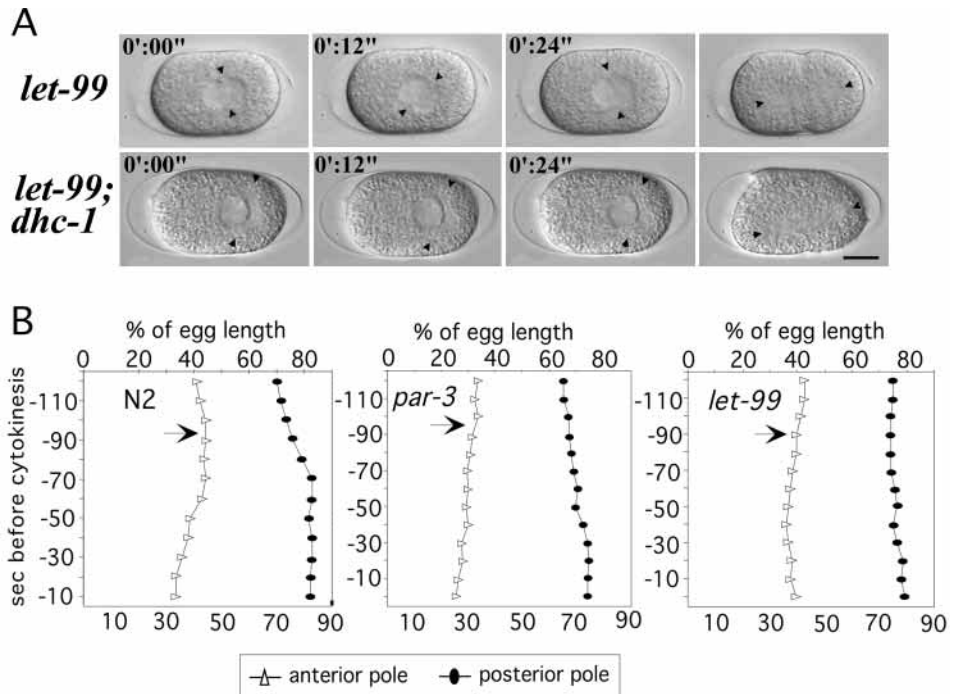


Fig. 1. Analysis of nuclear and spindle pole movements. (A) DIC images of live *let-99* (top row) and *let-99; dhc-1(RNAi)* (bottom row) embryos recorded by time-lapse video microscopy. Arrowheads mark the centrosomes and relative time points are indicated in the top left-hand corner of the images. Scale bar: 10 μ m. (B) Traces of spindle pole position in representative one-cell embryos from metaphase to cytokinesis onset (time 0). 0% egg length indicates the anterior tip of the embryo; the posterior tip would be at 100%. Arrows in wild type (N2) and *par-3* mark the time at which spindles began elongating and spindle poles started to oscillate; the most vigorous oscillations occurred in the middle of the elongation phase. Arrow in *let-99* indicates the time at which nuclear/spindle rocking ceased.

a 5' SL1 primer and a nested 3' *let-99* primer; products were cloned into pGEMT Easy. cDNAs and genomic DNA were sequenced using ABI automated sequencers (Cornell University Sequencing, Davis Sequencing).

RNA interference

Antisense and sense RNAs were transcribed in vitro from linearized cDNA templates (Ambion MEGAscript) using a full-length *let-99* cDNA, a *lrg-1* cDNA encoding amino acids 25-350, and the *dhc-1* cDNA yk161f11 (from Y. Kohara, National Institute of Genetics, Japan). Double-stranded RNA annealed as described elsewhere (Fire et al., 1998) was injected into adult hermaphrodites (1 mg/ml). Injection of single-stranded RNA was used for inhibition of *dhc-1* (1.5 mg/ml). The progeny of injected worms were analyzed 24-50 hours post-injection.

Antibodies and Immunolocalization

A fragment of a *let-99* cDNA, corresponding to amino acids 168-462, was cloned into the pMAL protein purification vector, expressed in bacteria, purified using amylose resin and injected into rabbits (Animal Resources Services, UC Davis). Antisera were purified using a GST:LET-99 fusion protein (pGEX) coupled to affigel. Western blotting was carried out as described previously (Basham and Rose, 2001), using dilutions of 1:3000 for LET-99 antibodies and 1:10,000 for tubulin DM1A (Sigma).

For in situ immunolocalization, worms were cut in egg buffer on poly-lysine coated slides, freeze-fractured, fixed with methanol and incubated with antibodies (anti-LET-99, 1:50; FITC-goat anti-rabbit, 1:200 in PBS) (see Miller and Shakes, 1995). Primary and secondary antibodies were pre-absorbed with acetone powders of GST-expressing bacteria and wild-type worms respectively. Single-section confocal images (mid-embryo focal plane) were analyzed using IP Images software (Scanalytic). Using the segmentation tool, the minimum pixel value displayed was increased until only the posterior band was labeled, thus defining the band, anterior and posterior domains. To quantify staining intensity, the line tool was used to mark the cortex, and the average pixel value of the marked region was measured. The unit of relative intensity in all tables is expressed as a ratio of peripheral staining to cytoplasmic staining (cytoplasmic values were obtained from the area beneath the cortex excluding the

nuclei and asters). Embryos were staged by DAPI (4',6-diamidino-2-phenylindole dihydrochloride) staining of the nuclei.

Microscopy and analysis of living embryos

Embryos were mounted to avoid flattening the embryo and examined under DIC optics using time-lapse video microscopy (Rose and Kempfues, 1998a). Centrosome movements were quantified by measuring the angular velocity of the nuclear-centrosome complex, which was then converted to a linear velocity using the radius of the complex. Spindle length was determined by measuring the distance between the spindle poles at metaphase (just after nuclear envelope breakdown) and at cytokinesis onset (first ingression of the cleavage furrow). To generate embryos with lateral or posterior meiosis, N2 males were mated to *fem-3* homozygous females as described elsewhere (Goldstein and Hird, 1996). To produce spherical embryos, embryos were treated with 1% hypochlorite, 0.5% KOH for 2 minutes and rinsed twice in egg buffer. Embryos were then mounted in a drop of chitinase (Hyman and White, 1987; Wolf et al., 1983) and examined by time-lapse from pronuclear formation through second cleavage, during which time eggshell digestion and rounding of the embryo occurred. Embryos remained fixed to the coverslip, allowing accurate determination of the axis defined by the initial position of the sperm nucleus.

RESULTS

let-99 mutants exhibit hyperactive nuclear movements and abnormal anaphase spindle pole behavior

It has previously been reported that *let-99* embryos exhibit an abnormal oscillation of the nuclear-centrosome complex, referred to as nuclear rocking (Rose and Kempfues, 1998a), instead of the normally smooth anterior centration and rotation observed in wild-type embryos. This rocking is an indication of the forces acting on centrosomes; we therefore quantified centrosome movements in one-cell embryos using time-lapse video microscopy (Fig. 1A, Table 1). The movement of the

Table 1. Centrosome movements and spindle pole separation in one-cell embryos

Hermaphrodite genotype	Speed of nuclear rotation/rocking ($\mu\text{m}/\text{second}$)*	Spindle length at metaphase [†]	Spindle length at telophase [†]	<i>n</i> [‡]
Wild type	0.09 \pm 0.03	32.2 \pm 1.6%	49.4 \pm 1.2%	10
<i>let-99</i>				
<i>it141/it141</i>	0.57 \pm 0.12	32.9 \pm 2.1%	39.3 \pm 1.4 %	8
<i>or81/or81</i>	0.59 \pm 0.07	31.7 \pm 1.6%	39.0 \pm 0.9%	9
<i>par-3</i>				
<i>it71/it71</i>	N/D	32.3 \pm 1.4%	49.1 \pm 1%	12
<i>par-3; let-99</i>				
<i>it71/it71; it141/it141</i>	N/D	32.5 \pm 1.5%	40.5 \pm 1.4%	8

*Based on measurements of videotaped embryos as described in Materials and Methods. The speeds shown for wild type and *let-99* are for nuclear rotation and rocking, respectively.
[†]Expressed as percentage of the egg length (calculated by dividing spindle length by embryo length)
[‡]Number of embryos.
N/D, not determined.

centrosomes during nuclear rocking in *let-99* embryos was about seven times faster than the movement of centrosomes during wild-type nuclear rotation. Furthermore, nuclear movements were not oriented along the AP axis, but could occur in any direction. The only motor protein known to be required for force generation during nuclear rotation in *C. elegans* is dynein (Gönczy et al., 1999). Thus, we tested whether dynein is required for the excessive nuclear movements observed in *let-99* embryos. RNAi interference (RNAi) of the dynein heavy chain gene (*dhc-1*) in wild type, using single-stranded RNA, results in normal nuclear migration and formation of a robust bipolar spindle of normal length, but a failure of centration and rotation (Gönczy et al., 1999). In *let-99; dhc-1(RNAi)* embryos, centration and nuclear rotation also failed, but the nuclear rocking phenotype was completely suppressed ($n=7$; Fig. 1A). Together, these results suggest that *let-99* embryos have alterations in cortical forces: instead of the wild-type asymmetric forces that produce centration and rotation, *let-99* embryos exhibit an increase in the net forces acting on the nuclear-centrosome complex and those forces appear randomly oriented.

The nuclear rocking behavior in *let-99* embryos continued during nuclear envelope breakdown and formation of a bipolar spindle, but then stopped abruptly. By contrast, in wild-type embryos the spindle poles are stationary until anaphase, when the elongation of the spindle begins. At this time, the posterior spindle pole exhibits lateral oscillations, also called spindle pole rocking (Albertson, 1984; Grill et al., 2001). To compare *let-99* and wild-type embryos further during anaphase, we tracked the movements of each spindle pole. In all wild-type embryos during the first half of anaphase, the posterior spindle pole moved towards the posterior end of the embryo while the anterior spindle pole remained stationary or moved posteriorly. Posterior spindle pole oscillations began just after the onset of spindle pole separation ($n=10$; Fig. 1B, left). By contrast, in *let-99* embryos posterior pole oscillations were reduced or absent and the spindle poles elongated symmetrically ($n=8$; Fig. 1B, right). This symmetric spindle elongation was similar to that in *par-3* mutant embryos (Fig. 1B, middle), where cortical forces during anaphase are uniform (Grill et al., 2001). In addition, in *let-99* embryos the extent of spindle pole separation was greatly reduced compared with both wild-type

and *par-3* embryos (Table 1). However, because the starting position of the spindle is more posterior in *let-99* embryos, owing to defects in centration (Rose and Kemphues, 1998a), cleavage is still unequal in these embryos. We conclude that LET-99 is required for asymmetric spindle pole movements during anaphase. In wild-type embryos, the forces that drive these asymmetric spindle pole movements appear to rely on interactions between the astral microtubules and the cortex, as well as on polarity cues (Bowerman and Shelton, 1999; Cheng et al., 1995; Gotta and Ahringer, 2001a; Grill et al., 2001; Rose and Kemphues, 1998b). Thus these results, together with the observations on nuclear rocking, suggest that LET-99 directly or indirectly regulates force generation between the cortex and the centrosomes to produce asymmetric movements.

The *let-99* gene encodes a novel DEP domain-containing protein

We identified the *let-99* gene using a combination of mapping, transformation rescue and RNA interference (Fig. 2A-C). Confirmation of the identity of the *let-99* gene came from sequencing three mutant alleles, all of which are nonsense mutations (Fig. 2D). Previous genetic analysis (Rose and Kemphues, 1998a) and comparison of the phenotypes produced by these mutations to that produced by RNA interference (Table 2) indicates that all three mutations produce a strong or complete loss of function. Analysis of cDNA and genomic sequence confirmed the exon/intron structure predicted by The *C. elegans* Sequencing Consortium (The *C. elegans* Sequencing Consortium, 1998) for open reading frame K08E7.3 (Fig. 2C) and indicated that the *let-99* transcript can be SL1 spliced. The predicted 698 amino acid LET-99 polypeptide (Fig. 2D) contains an N-terminal DEP domain (domain in Dishevelled, Egl-10 and Plekstrin) (Bateman et al., 1999; Ponting and Bork, 1996; Schultz et al., 2000). Because many DEP-containing proteins function with trimeric or small G proteins (Ponting and Bork, 1996; Schultz et al., 2000), the presence of the DEP domain supports the hypothesis that LET-99 functions as part of the G-protein signaling pathway that controls spindle position (Gotta and Ahringer, 2001b; Zwaal et al., 1996). Although database searches (Altschul et al., 1997) revealed no significant overall homology to proteins of known function, the *C. elegans* genome contains one *let-99* related

Fig. 2. Molecular identification of the *let-99* gene. (A) Genetic and physical maps of the region containing *let-99* on chromosome IV. (B) Restriction map and rescue data for cosmid C13H6 and fragments. (C) Restriction map and transcribed regions present in the smallest rescuing fragment. Northern blot analysis identified a 2.4 kb transcript that was expressed at high levels in the germline (*let-99*, open boxes) and two other transcripts (arrows), the positions of which were determined by the Genome Consortium (Genome Consortium, 1998). Injection of RNA corresponding to the 2.4 kb transcript into wild type resulted in a phenocopy of the *let-99* mutant phenotype in progeny embryos. (D) The predicted LET-99 and LRG-1 proteins, showing the positions of *let-99* mutations and the corresponding amino acids change. The DEP domain is boxed; shaded box indicates a block of amino acids (153-212) present in LET-99 but not LRG-1; LRG-1 is 86% identical to the N-terminal region of LET-99. The Genbank Accession Number for *let-99* (K08E7.3) is Z77666 and for *lrg-1* (F55H2.4) is NP_499092. (E) Western blot of wild-type (N2) and *let-99(or81)* mutant embryos probed with affinity-purified anti-LET-99 antibodies and re-probed with anti-tubulin as a loading control.

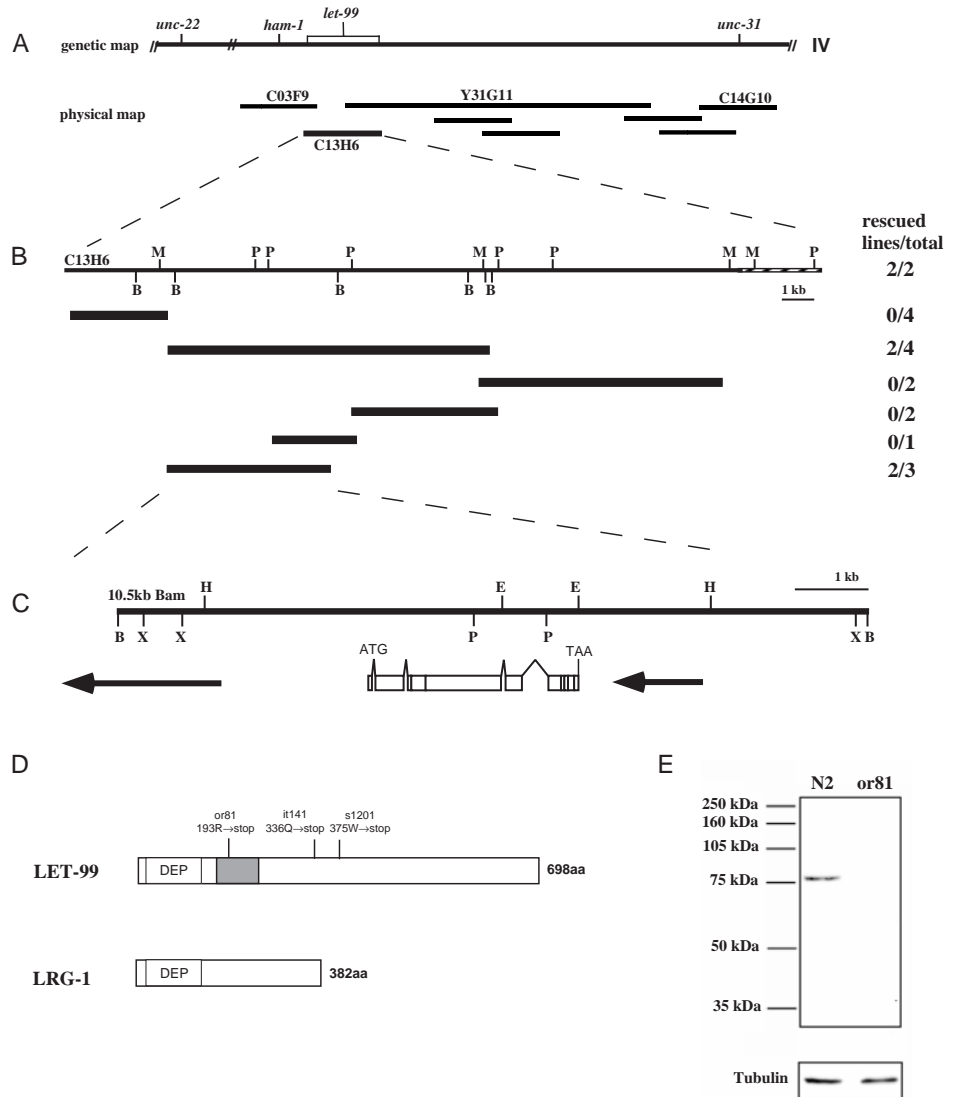


Table 2. Analysis of meiosis and spindle orientation

Genotype	Number of embryos with phenotype described							
	Two polar bodies*	First cleavage: rotation angle at NEBD [†]			Second cleavage [‡] :			
		<30	30-60	60-90				
Wild type	25/25	11	1	0	12	0	0	0
<i>let-99(or81)/(or81)</i>	20/20	5	12	2	0	14	5	0
<i>let-99(it141)/(it141)</i> [§]	ND	9	6	3	0	10	7	2
<i>let-99(it141)/sDf22</i> [§]	ND	0	4	6	0	8	6	0
<i>let-99(RNAi)</i> [¶]	ND	4	12	3	0	1	9	0
<i>lrg-1(RNAi)</i> [¶]	10/10	5	11	4	0	11	6	3
<i>let-99;lrg-1(RNAi)</i>	10/10	5	12	2	0	9	9	0

*DAPI stained one and two-cells embryos scored for polar bodies. Extra pronuclei were never observed by DAPI or DIC imaging in any of the genotypes.

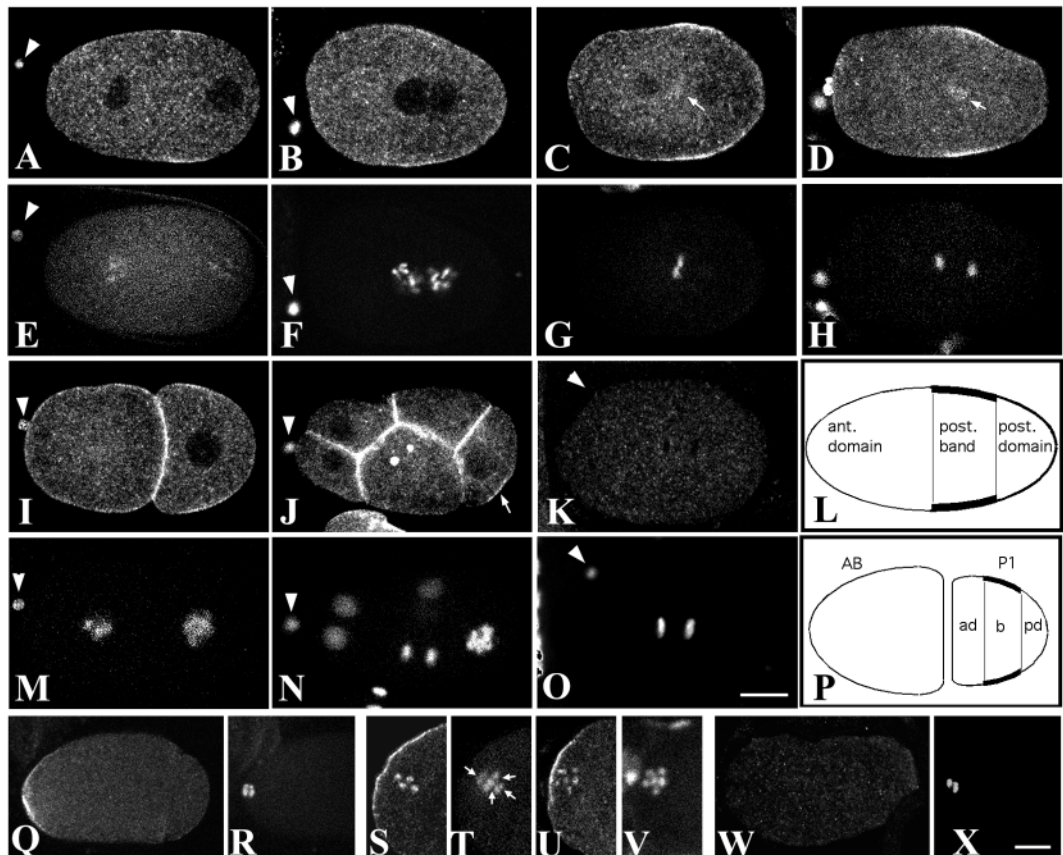
[†]Angle of a line drawn between the two centrosomes relative to the anterior/posterior axis (0°) at the time of pronuclear envelope breakdown as visualized by DIC microscopy.

[‡]Scored as in Rose and Kemphues (Rose and Kemphues, 1998a).

[§]Data taken from Rose and Kemphues (Rose and Kemphues, 1998a).

[¶]Immunolocalization experiments showed that LET-99 protein was absent in *let-99(RNAi)* and in *lrg-1(RNAi)* embryos. The latter suggests that the phenotypes of *lrg-1(RNAi)* embryos are due to cross-interference (Fire et al., 1998) with *let-99*.

Fig. 3. Immunolocalization of the LET-99 protein in one-cell embryos. Confocal sections of mitotic stage wild-type embryos (A-J, M-N) and *let-99 (or81)* embryos (K, O) and meiotic stage wild-type (Q-V) and *let-99 (or81)* (W, X) embryos stained with affinity-purified LET-99 antibodies (A-D, I-K, Q, S, U, W) and DAPI (E-H, M-O, R, T, V, X). Anterior is towards the left in this and all subsequent figures unless indicated. (A, E) Early prophase embryo during pronuclear migration. (B, F) One-cell prophase embryo during centration, before nuclear rotation has occurred. (C, G) One-cell metaphase embryo. (D, H) One-cell anaphase embryo. (I, M) Two-cell embryo in which P₁ is in prophase. (J, N) Six-cell embryo in which P₂ is in prophase. (K, O) One-cell *let-99* anaphase embryo. Arrowheads indicate polar bodies that are positive for LET-99 staining in wild-type



embryos and negative for LET-99 in mutant embryos. Arrows in C, D indicate the metaphase plate- (C) and the spindle midzone- (D) associated staining of LET-99. Arrow in J indicates the LET-99 band in the P₂ cell. (L, P) Schematic diagram of one-cell and two-cell embryos showing the three LET-99 domains in P lineage cells: anterior domain, posterior band and posterior domain. (Q, R) Wild-type embryo in anaphase of meiosis. (S, T) Wild-type embryo in metaphase of meiosis viewed from the side; the spindle axis is parallel to the edge of the embryo and tilted slightly towards viewer. arrows in T indicate faint gaps in DAPI staining between opposed chromatin masses to which the bars of LET-99 appear to localize. Such gaps and corresponding LET-99 bars were visible in meiotic prometaphase as well. (U, V) Wild-type embryo in meiosis viewed from one spindle pole. (W, X) *let-99 (or81)* embryo in anaphase of meiosis. Scale bars: in O, 10 μ m for A-O; in X, 10 μ m for Q-X.

gene (*lrg-1*) that is highly similar at the nucleotide level to the entire *let-99* transcribed region, but encodes a truncated protein (Fig. 2D). RNA interference experiments revealed no additional role for *lrg-1* in the early embryo (Table 2), suggesting that there is no redundancy between *lrg-1* and *let-99* for spindle positioning.

LET-99 is enriched asymmetrically at the cell periphery in the P lineage

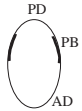

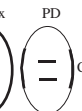

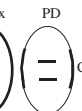
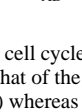
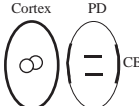
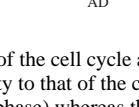
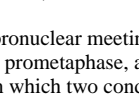
One way in which LET-99 could function to regulate forces asymmetrically is for the LET-99 protein itself to be asymmetrically localized. We carried out in situ immunolocalization experiments using affinity purified antibodies specific for the LET-99 protein (Fig. 2E, Fig. 3) to determine the localization of LET-99 in embryos. LET-99 was present in the cytoplasm and asymmetrically enriched at the cell periphery during both meiosis and mitosis. All of the patterns described are specific to LET-99, as evidenced by their absence in *let-99* mutant embryos (Fig. 3K, W). However, as described below, the asymmetric peripheral enrichment of LET-99 during early cleavage correlates with polarized nuclear and spindle movements in wild-type and mutant embryos.

In wild type, LET-99 was first observed during meiosis I and

II where it was asymmetrically localized to the anterior periphery near meiotic spindles (37/44 embryos; Fig. 3Q, R); both polar bodies were positive for LET-99 in later embryos (Fig. 3A, E). In embryos in which meiosis occurred laterally or at the posterior pole (Goldstein and Hird, 1996), LET-99 was always associated with the periphery adjacent to the meiotic spindle ($n=9$). Thus, LET-99 is localized near the meiotic spindle and not to the anterior of the embryo per se. In addition, LET-99 was observed between opposed chromatin masses in metaphase and in the spindle midzone at anaphase during meiosis (Fig. 3Q-V) and mitosis (Fig. 3C, D, G, H). During mitosis, a slight enrichment of LET-99 in the cytoplasm around nuclei and microtubule asters was also seen. However, no gross defects in mitosis, meiosis or polar body formation were observed in *let-99* mutants or *let-99(RNAi)* embryos, and no redundancy of *lrg-1* for meiosis or mitosis was revealed by RNA interference (Table 2, data not shown) (Rose and Kemphues, 1998a). Thus, while the peripheral localization of LET-99 during meiosis is the earliest marker for the region that anchors the meiotic spindle, the role of this and the chromosome/spindle associated LET-99 remains to be elucidated.

In mitotic-stage wild-type embryos, LET-99 was

Table 3. Quantification of LET-99 staining intensity in one-cell embryos

Genotypes/domains	Relative intensity and range of LET-99 domains at different cell cycle stages*		
	Prophase [†]	Metaphase [‡]	Late anaphase [§]
Wild type (N2)			
Posterior domain (PD)	<i>n</i> =16 1.10±0.11	<i>n</i> =23 1.46±0.23	<i>n</i> =8 1.05±0.16
Posterior band (PB)	1.46±0.15	2.21±0.52	2.31±0.31
Anterior domain (AD)	1.02±0.11	1.17±0.15	1.23±0.19
PB range	50.6±5.6 to 73.5±6.4%	48.2±3.3 to 71.2±4.1%	48.9±3.7 to 73.2±4.8%
<i>par-2 (lw32/lw32)</i>			
Posterior domain (PD)	<i>n</i> =5 1.46±0.13	<i>n</i> =10 1.81±0.29	<i>n</i> =3 1.84±0.12
Anterior domain (AD)	1.0±0.15	1.34±0.23	1.29±0.10
PD range	71.3±8.0 to 100%	67.6±7.2 to 100%	60.9±8.6 to 100%
<i>par-3 (it71/it71)</i>			
Cortex/central Band (CB)	<i>n</i> =9 1.26±0.1	<i>n</i> =14 1.94±0.36	<i>n</i> =7 2.24±0.33
Posterior (PD)	N/A	N/A	1.67±0.27
Anterior (AD)	N/A	N/A	1.65±0.33
CB range	N/A	N/A	31.4±6.1 to 63.6±5.4%

*Embryos were grouped by stages of the cell cycle as indicated below, based on DAPI staining, for ease of comparison. Relative intensity in all embryos is a ratio of the peripheral staining intensity to that of the cytoplasm. The high standard deviation appears to result from grouping embryos into discontinuous categories (e.g. prophase versus metaphase) whereas the staining intensity of LET-99 appears to more continuously change (e.g. increasing from early prophase to metaphase/anaphase).

[†]Prophase includes embryos from pronuclear meeting to before nuclear envelope breakdown (NEBD).

[‡]Metaphase includes embryos from prometaphase, as judged by NEBD, to metaphase.

[§]Late anaphase includes embryos in which two condensed, clearly separated DNA masses were present.

N/A, not applicable.

asymmetrically enriched at the cell periphery, beginning at pronuclear migration in the one-cell embryo (Fig. 3A-D, Table 3). The areas enriched for LET-99 encircled the posterior of the embryo but did not include the entire pole, and will be referred to as posterior bands; one-cell embryos thus exhibited three distinct regions of LET-99 staining: the anterior domain, the posterior band and the posterior domain (Fig. 3L). The posterior bands were asymmetrically positioned at all stages; for example, in embryos at nuclear rotation stage, the posterior band extended from 51-74% egg length (Table 3, Fig. 3B). Quantification of average fluorescence intensity confirmed that the highest staining intensity was in the posterior band at all stages and that the intensity increased during the cell cycle (Table 3). In late anaphase embryos, a strong LET-99 band was still present, but the staining intensity of the posterior domain diminished (Fig. 3D, Table 3).

At the two-cell stage, LET-99 was enriched in a band at the cell periphery of P1 at all stages of the cell cycle (*n*=47; Fig. 3I and not shown). While the cell-cell contact region also appeared enriched for LET-99, quantification revealed this region had a staining intensity consistent with the juxtaposition of the AB and P1 membranes (Table 4). Thus, LET-99 appears to be present in three domains at the cell periphery in P1 just as in the one-cell embryo (Fig. 3P). During third cleavage, LET-99 was enriched in a peripheral band in P2 (Fig. 3J; *n*=15), and the band was in a position consistent with the reversal of polarity exhibited by this cell (Schierenberg, 1987). In contrast to the P lineage cells, the AB cells and EMS had symmetric distributions of LET-99 at all times (*n*=43). Peripheral LET-99 became weaker in later embryos, disappearing between the 28-cell and the 50-cell stage. From these observations, we conclude that LET-99 is present at the cell periphery in all cells, but that P cells exhibit a dynamic asymmetric enrichment of LET-99.

Asymmetric enrichment of LET-99 depends on the *par* genes

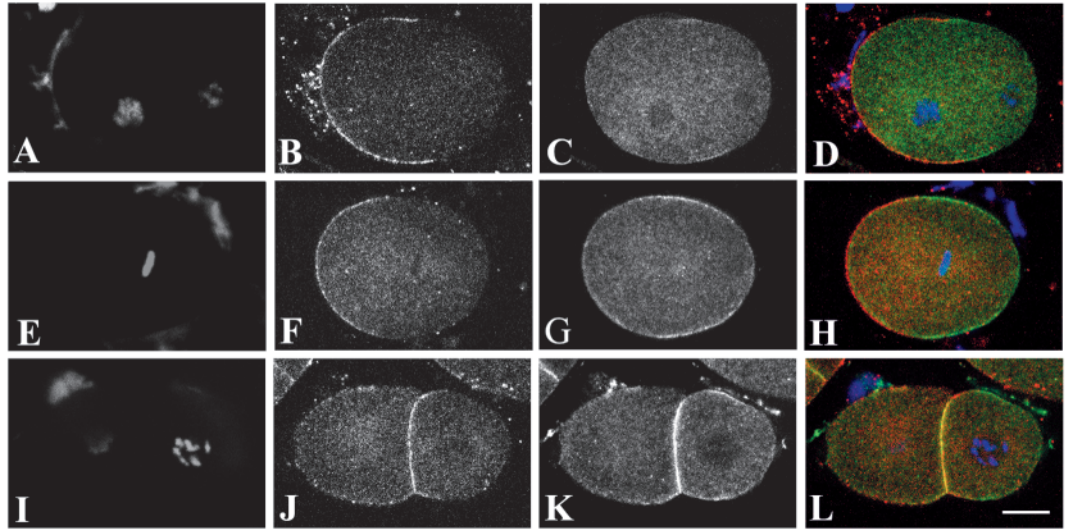
The asymmetric distribution of LET-99 along the AP axis suggests that LET-99 may be localized in response to polarity cues. The PAR-3 and PAR-2 proteins are localized to apparently non-overlapping anterior and posterior peripheral domains respectively in both the one-cell and P1 cell embryo (reviewed in Bowerman and Shelton, 1999; Rose and Kemphues, 1998b). To determine the relationship of the LET-99 posterior band to these domains, wild-type

Table 4. Quantification of LET-99 staining intensity in two-cell embryos

Genotype and domain	Relative intensity to cytoplasm
Wild-type (N2)	<i>n</i> =11
Posterior domain (PD)	1.36±0.18
The LET-99 band (B)	2.26±0.28
Anterior domain (AD)	1.51±0.23
Cell/cell contact (CC)	3.08±0.33
AB cortex	1.60±0.24
<i>par-2 (lw32/lw32)</i>	<i>n</i> =6
P1 cortex	1.65±0.15
Cell/cell contact	3.63±0.71
AB cortex	1.33±0.19
<i>par-3 (it71/it71)</i>	<i>n</i> =7
Cortex (CX)	1.81±0.29
Cell/cell contact	2.85±0.43

Only embryos in which the P1 cell (wild type) or both cells (*par* mutants) were in late prophase were used in this analysis. In wild-type embryos, the AB cell was in prometaphase/metaphase at this time. Late prophase included embryos in which chromosomes were highly condensed but nuclear envelope breakdown had not occurred, as judged by DAPI staining. As in one-cell embryos, staining intensity increased during cell cycle in both AB and P1.

Fig. 4. Comparison of LET-99 and PAR-3 staining in wild-type embryos. Confocal micrographs of wild-type embryos triple labeled with DAPI (A, E, I), anti-PAR-3 (B, F, J) and anti-LET-99 antibodies (C, G, K). Merged images (D, H, L) show PAR-3 in red, LET-99 in green and DNA in blue. (A-D) 1-cell embryo during pronuclear migration. (E-H) 1-cell metaphase embryo. (I-L) 2-cell embryo in which P1 is in late prophase. The focal plane was chosen to show the P1 cell most clearly. Scale bar: 10 μ m.



embryos were double-labeled with antibodies against PAR-3 and LET-99. In all one-cell embryos, the region of high LET-99 staining intensity that defines the band was directly adjacent to, but did not appear to overlap with, the posterior edge of the PAR-3 domain (Fig. 4A-H; $n=8$ prophase, $n=7$ metaphase and $n=4$ anaphase embryos). A similar relationship was observed between the LET-99 band and the edge of the PAR-3 domain in the P1 cell at the two-cell stage (Fig. 4I-L; $n=9$). Thus, the anterior domain of low LET-99 staining intensity appears coincident with the PAR-3 domain, while the posterior band and posterior domain of LET-99 together occupy the same region as the PAR-2 domain.

To test the hypothesis that the distribution of LET-99 depends on PAR cues, we analyzed the pattern of LET-99 localization in both *par-3* and *par-2* embryos. In one-cell *par-3* embryos, LET-99 was present around the entire periphery in all prophase through metaphase stage embryos ($n=31$; Fig. 5A,B). The staining intensity at the periphery was comparable with that of the posterior band of wild-type embryos (Table 3). During anaphase, the LET-99 signal at the anterior and posterior of one-cell *par-3* embryos diminished, leaving a band of LET-99. However, in contrast to wild type, this band was symmetrically positioned and will be referred to as the central band ($n=13$; Fig. 5C). In *par-2* one-cell embryos, two LET-99 domains were observed (Fig. 5I-K, Table 3). The anterior domain in *par-2* embryos had low LET-99 staining intensity as in wild type, but was expanded to include part of the region normally covered by the posterior band. The posterior domain had a staining intensity of LET-99 similar to the wild-type posterior band. Two domains were observed at anaphase as well. This altered LET-99 distribution pattern in *par-2* embryos correlates with the changes in PAR-3 distribution previously described. Although PAR-3 extends around the entire periphery in *par-2* one-cell embryos, there is a gradient from high levels of PAR-3 at the anterior to lower levels at the posterior (Boyd et al., 1996; Etemad-Moghadam et al., 1995). These results show that the pattern of LET-99 localization in one-cell embryos depends on the PAR proteins and further that higher levels of PAR-3 correlate with lower levels of LET-99 in

prophase through metaphase embryos. The specific cues that differentiate the posterior band from the posterior domain remain to be determined.

LET-99 was also mislocalized in two-cell *par* mutant embryos. In *par-3* embryos, LET-99 was present around the entire periphery of both the AB and P1 cells in prophase through metaphase ($n=38$; Fig. 5D), but then localized to a central band in both cells during anaphase ($n=10$). In *par-2* two-cell embryos LET-99 localization at the periphery of both cells appeared uniform at all stages of the cell cycle (Fig. 5L). Although no bands were observed in either *par* mutant during prophase, the staining intensity of peripheral LET-99 was higher in *par-3* two-cell embryos than in *par-2* embryos (excluding the cell contact region; Table 4). In contrast to changes in peripheral LET-99 localization, the localization of LET-99 to the metaphase plate and anaphase spindle midzone in *par-2* and *par-3* embryos was comparable with wild type (Fig. 5B,C,J,K). Therefore, the one-cell and two-cell data indicate that asymmetric enrichment of LET-99 at the periphery is polarity dependent, and supports the hypothesis that LET-99 acts downstream of the PAR-3 and PAR-2 proteins.

Nuclear rotation fails in spherical *par-3* 1-cell embryos

If peripherally localized LET-99 functions as an intermediate to translate polarity cues into spindle orientation, then the pattern of LET-99 should correlate with nuclear rotation in *par* embryos as in wild type. In *par-2* mutants, the mislocalization of LET-99 correlates with defects in nuclear rotation. In approximately half of *par-2* one-cell embryos, the first spindle does not align on the AP axis before anaphase, and in virtually all *par-2* two-cell embryos there is no nuclear rotation in P1 (data not shown) (Cheng et al., 1995). However, no defects in nuclear rotation have been reported for *par-3* one-cell embryos (Cheng et al., 1995; Kirby et al., 1990), where LET-99 is symmetrically distributed around the periphery during prophase. We re-examined *par-3* 1-cell embryos and also observed rotation of the nuclear-centrosome complex onto the AP axis during prophase ($n=13$ 1-cells); however, as previously noted (Kirby et al., 1990), the pronuclei meet more centrally

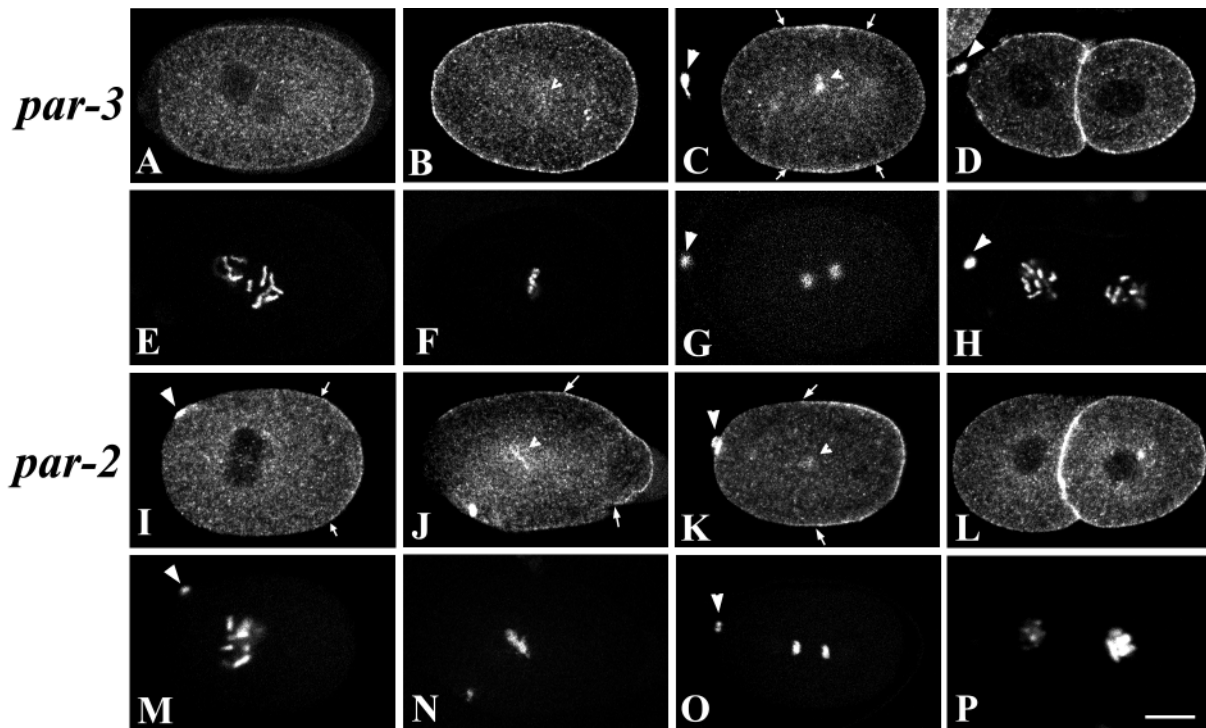


Fig. 5. LET-99 localization depends on PAR-3 and PAR-2. Confocal images of *par-3* embryos (A-H) and *par-2* embryos (I-P) stained with anti-LET-99 antibodies (top panels) and DAPI (bottom panels). (A,E,I,M) One-cell prophase embryos. (B,F,J,N) One-cell metaphase embryos. (C,G,K,O) One-cell late anaphase embryos. (D,H,L,P) Two-cell prophase embryos. Arrows indicate the boundaries of the LET-99 central band in *par-3* and of the posterior domain in *par-2* embryos. Large arrowheads indicate polar bodies. Small arrowheads in B,J and C,K indicate the metaphase plate and spindle midzone-associated staining of LET-99, respectively; the intensity of these two patterns varies in both wild type and *par* mutants. Scale bar: 10 μ m.

in *par-3* embryos and thus centration is not comparable with wild type.

Although no intrinsic asymmetries appear to be present in *par-3* embryos (Bowerman and Shelton, 1999; Rose and Kemphues, 1998b), one obvious extrinsic asymmetry is the oblong shape of the egg itself. To test the hypothesis that nuclear rotation in *par-3* embryos is due to egg shape rather than the normal rotation mechanism, we examined embryos in which the eggshell was removed by chitinase digestion. As reported previously (Hyman and White, 1987), nuclear rotation still occurred in wild-type embryos that rounded up completely before rotation began ($n=3$; Fig. 6); this indicates that the spindle oriented with respect to the intrinsically polarized axis defined by the sperm's position. By contrast, in spherical *par-3* embryos, no nuclear rotation occurred and the spindle set up on a transverse axis ($n=6$; Fig. 6). In *par-3* embryos in which the embryo rounded up during nuclear rotation, rotation stopped and the spindle set up on an oblique axis ($n=5$). Interestingly, in two additional cases in which the sperm was positioned laterally and the embryo was still oblong, the spindle oriented with respect to the long axis, rather than with the axis defined by sperm position. In addition, in all of these spherical *par-3* embryos, both spindle poles oscillated during anaphase, and at the two-cell stage the spindles in both cells aligned towards the cell contact region, as in untreated *par-3* embryos. We conclude that in *par-3* one-cell embryos, the extrinsic asymmetry of the oblong egg results in nuclear rotation. The *par-3* phenotype is thus

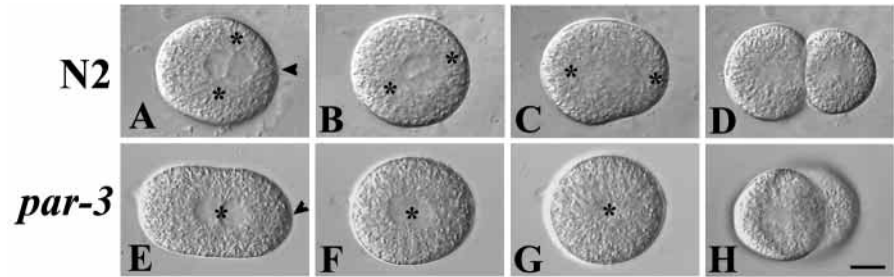
consistent with the hypothesis that the LET-99 band plays a role in normal nuclear rotation. Furthermore, these results suggest that in *par-3* embryos there is no remaining polarity at the one-cell stage (e.g. dictated by oocyte polarity or sperm position) that specifies anaphase spindle pole oscillations or two-cell spindle alignment, because these movements occurred regardless of first cleavage orientation. The cue for spindle alignment in two-cell *par-3* embryos is likely to be the cell contact region itself (Skop and White, 1998; Waddle et al., 1994).

Although all *let-99* one-cell embryos display nuclear rocking and centration defects, only half fail to align the nuclear-centrosome complex during prophase (Rose and Kemphues, 1998a). To determine if spindle alignment in these embryos is due to cell shape, as in *par-3* mutants, we examined chitinase-digested *let-99* embryos. In eight out of eight spherical embryos, nuclear rotation failed completely and the nuclear-centrosome complex rocked vigorously. Taken together with the *par-3* data, these results suggest that LET-99 and its asymmetric distribution are essential for normal nuclear rotation in one-cell embryos.

LET-99 is required for ectopic anaphase spindle pole oscillations in *par-3* embryos

We also examined whether LET-99 asymmetry correlates with anaphase spindle pole movements in *par-3* mutants. In *par-3* embryos, the central band of LET-99 seen at anaphase correlates with the oscillation of both spindle poles and

Fig. 6. Nuclear rotation fails in spherical *par-3* one-cell embryos. DIC images of live wild-type (A-D) and *par-3* (E-H) embryos during chitinase treatment to remove the eggshell. Arrowheads mark the position of the sperm pronucleus before nuclear migration. Asterisks indicate the centrosomes. In the *par-3* embryo, the two centrosomes are aligned into the plane of the image, transverse to the axis defined by the position of the sperm, and thus only one centrosome is visible. Scale bar: 10 μ m.



symmetric spindle pole separation (Cheng et al., 1995). To test whether LET-99 is required for spindle pole oscillations in *par-3* embryos, we examined *par-3 let-99* embryos. Just as in *let-99* embryos, nuclear and metaphase rocking was observed, but stopped abruptly during anaphase; no spindle pole oscillations were observed, and spindle pole separation was reduced ($n=8$, Table 1). This data, together with the *let-99* single mutant phenotype, suggests that the LET-99 band plays a role in spindle pole oscillations.

DISCUSSION

LET-99 functions as an intermediate in the PAR pathway for spindle positioning

In wild-type embryos, AP polarity is established and maintained by PAR proteins, which are asymmetrically localized in response to a cue from the sperm (Bowerman and Shelton, 1999; Goldstein and Hird, 1996; Gotta and Ahringer, 2001a; Wallenfang and Seydoux, 2000). Previous work showed that *let-99* plays a role in spindle orientation but not polarity (Rose and Kemphues, 1998a). The studies presented here provide several new lines of evidence that LET-99 functions as a key intermediate in the PAR pathway to determine spindle position. First, LET-99 is asymmetrically enriched at the periphery of the P lineage cells in a unique band pattern that is PAR-3 and PAR-2 dependent. Second, the asymmetric enrichment of LET-99 at the periphery correlates with nuclear centration/rotation and anaphase spindle positioning in the one-cell and P₁ cell of wild-type embryos and with defects in these movements in *let-99* embryos. Third, the altered distribution of LET-99 in *par-3* and *par-2* mutant embryos correlates with changes in nuclear rotation and anaphase spindle positioning seen at the one-cell stage in these mutants. These data provide strong evidence that asymmetric enrichment of LET-99 at the periphery determines several aspects of spindle positioning in response to polarity cues.

A model for LET-99 function in the 1-cell embryo

The current model for nuclear and spindle positioning in *C. elegans* embryos is that the asymmetric PAR protein domains lead to asymmetric cortical forces that control nuclear and spindle movements (Gotta and Ahringer, 2001a; Rose and Kemphues, 1998b). However, it appears that the net forces acting on the centrosomes during nuclear centration/rotation (anteriorly directed) are opposite to those acting during anaphase spindle positioning (posteriorly directed). Thus, it is unclear how the same PAR domains could result in oppositely oriented forces.

The unique enrichment of LET-99 in a posterior band provides a model that simplifies this apparent paradox. The hyperactive dynein-dependent movement of the nuclear-centrosome complex in *let-99* mutants suggests that the ultimate effect of LET-99 activity is a net inhibition of force generation between the cortex and astral microtubules (through several possible mechanisms). We thus propose that in wild type, the net force on the astral microtubules is lowest at regions enriched for LET-99 (Fig. 7A). A key feature of our model is that because of the geometry of centrosome position relative to the LET-99 band, the net forces produced on the centrosomes are different during centration/rotation and anaphase. Specifically, after pronuclear meeting the centrosomes are oriented transverse to the long axis of the embryo, parallel to the LET-99 band (Fig. 7A). Our model proposes that any small stochastic shift in centrosome position that places one centrosome more anterior (and thus more astral microtubules outside of the LET-99 band) would result in a net anterior force on that centrosome (Fig. 6A, red arrows). The band would similarly result in net posterior force on the other centrosome and thus create rotational torque. By contrast, during anaphase the centrosomes are aligned perpendicular to the LET-99 band. In early anaphase, the majority of anterior spindle pole astral microtubules are outside of the LET-99 band, which would result in radially uniform force on the spindle pole and the absence of anteriorly directed pole movements. By contrast, the posterior pole astral microtubules are partially in the LET-99 band; the inhibition of laterally directed forces in the band would produce a greater net posterior force on the spindle pole, causing posterior movement and lateral oscillations.

The model is consistent with the changes in nuclear rotation and anaphase spindle pole movements seen in *let-99* embryos and in one-cell *par* mutant embryos. Abnormal LET-99 localization correlates with defects in nuclear rotation in *par-2* embryos. Although nuclear rotation did occur in *par-3* embryos in which LET-99 is distributed uniformly around the periphery at prophase, our eggshell digestion experiments showed that this is not the normal rotation but is instead dictated by egg shape. Thus, these results also addressed the question of how nuclear rotation can occur in embryos that are presumed to lack all polarity. Furthermore, the central band of LET-99 observed at anaphase in *par-3* embryos correlates with spindle pole movements. In these embryos, astral microtubules from both spindle poles partially contact the LET-99 band, analogous to the posterior spindle pole in wild type (Fig. 7B). We propose that it is this positioning of spindle poles relative to the LET-99 band that causes both spindle poles to oscillate (Cheng et al., 1995) and to show posterior rates of movement

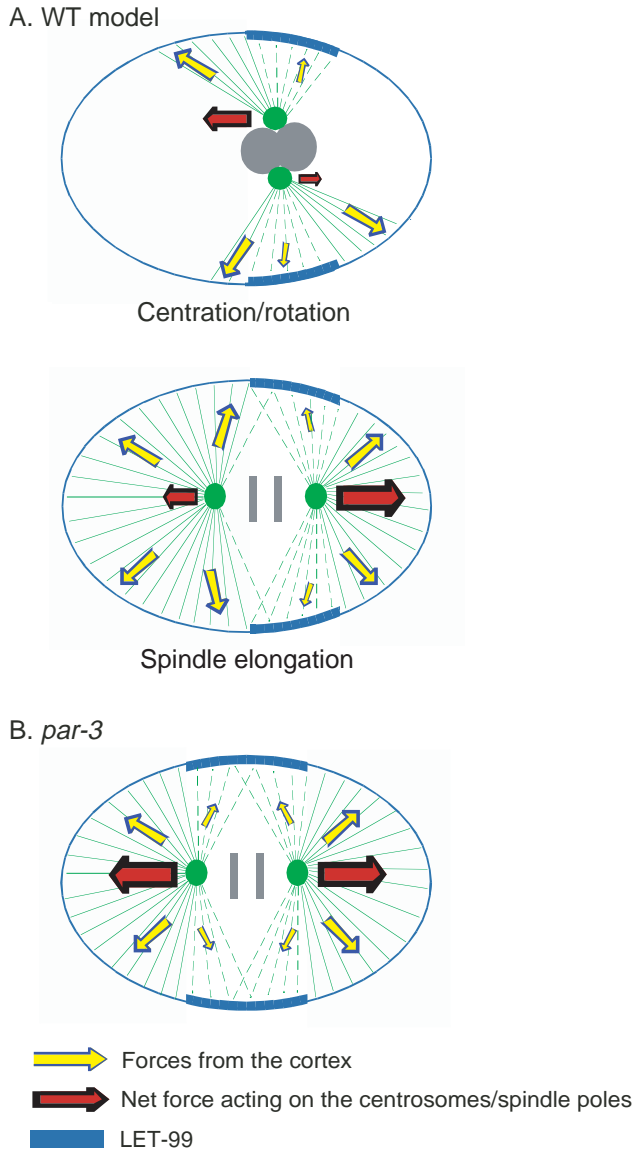


Fig. 7. Model for the role of LET-99 in nuclear rotation and anaphase spindle positioning in one-cell embryos. Anterior is towards the left. Centrosomes and microtubules are shown in green. Yellow arrows indicate forces from the cortex acting on subsets of astral microtubules. Broken lines indicate microtubules that contact regions enriched for LET-99 and experience less force (small yellow arrows; see text). Red arrows indicate the net force acting on the centrosomes or spindle poles, with size proportional to the magnitude of the force. (A) Prediction of forces during centration/nuclear rotation and anaphase spindle positioning in wild type. (B) Prediction of forces on spindle poles during anaphase in *par-3* mutant embryos.

(Grill et al., 2001). Finally, the model for LET-99 also fits well with the results of Grill et al. (Grill et al., 2001). They found that in mathematical models of spindle pole movements after severing the central spindle, neither an increase in force on all posterior astral microtubules nor an increase in the density of posterior microtubules reproduced all aspects of posterior pole behavior: speed, distance traveled and lateral oscillations. However, a model in which the lateral microtubules of the posterior aster detached from the cortex or became inactive as

they elongated during posterior displacement of the spindle pole was able to reproduce all three aspects. LET-99 is an excellent candidate for functioning in a pathway that results in such detachment/inactivation. Furthermore, the band localization of LET-99 could provide the cue for microtubules to be inactivated only laterally, and not throughout the entire posterior domain, in intact wild-type spindles.

In wild-type two-cell embryos, the asymmetric enrichment of LET-99 could function in a similar way to facilitate nuclear rotation and anaphase spindle positioning in P1. In *par-3* mutants, the banded pattern of LET-99 per se does not appear to be required for nuclear rotation in AB and P1. The cell contact/cell division remnant probably provides the asymmetric cue for nuclear rotation in *par-3* embryos. This region exhibits an enrichment of dynein/dynactin complex components and has been shown to be required for nuclear rotation in wild-type embryos (Gönczy et al., 1999; Skop and White, 1998; Waddle et al., 1994). Nonetheless, higher levels of LET-99 correlate with rotation in *par-3* two-cell embryos, while lower levels or the absence of LET-99 correlates with lack of rotation in *par-2* and *let-99* mutants. Thus, we speculate that there is a threshold level of LET-99 that is required to inhibit net forces enough to allow nuclear rotation. In wild-type embryos at the two-cell stage, the banded pattern of LET-99 is predicted to facilitate rotation in conjunction with the cue from the cell contact region/cell division remnant.

LET-99 may regulate forces on centrosomes as part of a G protein signaling pathway

At the molecular level, LET-99 could function to inhibit cortical forces through several microtubule-based processes that are not mutually exclusive. There are no gross abnormalities in microtubule organization in *let-99* mutant embryos (Rose and Kemphues, 1998) (data not shown). Nonetheless, LET-99 could inhibit dynein activity at the cortex, modify interactions between astral microtubules and the cortex, or cause changes in microtubule dynamics that are not detectable by conventional immunolocalization of tubulin. We found that reducing dynein activity suppressed the hyperactive rocking phenotype of *let-99* embryos. The genetic interpretation of this result is that in wild type, LET-99 inhibits dynein directly or indirectly, consistent with the model in which LET-99 downregulates dynein activity and thus force at the cortex. However, the suppression could also result from changes in microtubule dynamics or microtubule organization caused by lowered dynein activity (Gönczy et al., 1999) and thus is also consistent with LET-99 acting through dynein-independent mechanisms. Only a few other microtubule-associated proteins that influence spindle orientation have been identified (Gönczy et al., 2001; Matthews et al., 1998). These or other microtubule-associated proteins could be targets of LET-99 activity instead of or in addition to dynein, and the targets in theory could be different for anaphase versus nuclear rotation.

LET-99 has no recognizable domains for interacting directly with the cytoskeleton but does contain a DEP domain, a motif implicated in recruitment to the cell periphery and found in components of G protein signaling pathways (Axelrod et al., 1998; Schultz et al., 2000; Wong et al., 2000). Therefore, we postulate that LET-99 plays a regulatory role, potentially as part of the G protein signaling pathway described in *C. elegans* embryos (Gotta and Ahringer, 2001b; Zwaal et al., 1996),

rather than having a direct interaction with cytoskeletal proteins. The G proteins appear uniformly distributed; the distribution of LET-99 in response to PAR proteins could thus provide for asymmetric activation of the G proteins or asymmetric localization of effectors.

It has been found that trimeric G proteins and PAR-3 and its binding partners also play a role in asymmetric division in *Drosophila*. In that system, the G proteins function in localizing cell fate determinants in addition to orienting the spindle (reviewed by Doe and Bowerman, 2001; Knust, 2001). In *Drosophila*, the Inscuteable protein serves as the link between the polarity cues and the G proteins, as we have postulated for LET-99 in *C. elegans*. LET-99 and Inscuteable have no sequence similarity or shared domains, but could be functioning similarly as adaptor proteins to organize protein complexes. *Drosophila* does not appear to have an ortholog for LET-99, even in terms of domain organization, nor does *C. elegans* have a clear Inscuteable ortholog. This lack of conservation could in part be due to differences in embryonic development. In *C. elegans*, as in many other organisms, early divisions take place in large cells that require long astral microtubules to reach the cortex. In *Drosophila*, early divisions occur first in cytoplasmic islands and then in small membrane domains within the syncytial blastoderm; similarly, the asymmetric divisions that require Inscuteable occur in small cells (Doe and Bowerman, 2001; Knust, 2001). The strict maternal requirement for LET-99 (Rose and Kemphues, 1998a) suggests it is specialized for functioning in large embryonic cells. Both the mouse and human genomes encode several proteins with a similar domain organization as LET-99. It will be interesting to learn whether these DEP proteins function in any aspects of spindle positioning during the early development of these organisms.

We thank Alan Coulson for cosmid, Theresa Stiernagle (Caenorhabditis Genetics Center; which is funded by the NIH National Center for Research Resources) and Gian Garriga for strains, Yuji Kohara for cDNAs, Bob Barstead and Peter Okkema for cDNA libraries, and Susie Schmid and Christalynn Tan for technical assistance. L. R. is indebted to Ken Kemphues and members of his laboratory for strains, antibodies, discussions and support during the early stages of this work. We also thank Frank McNally, Ken Kaplan, Alan Rose and the reviewers for comments on the manuscript, and members of the Rose, McNally and Scholey laboratories for helpful discussions. This work was supported by a NIH Shannon's Director Award and an American Cancer Society Research Program Grant to L. R.

REFERENCES

- Albertson, D.** (1984). Formation of the first cleavage spindle in nematode embryos. *Dev. Biol.* **101**, 61-72.
- Altschul, S. F., Madden, T. L., Schaffer, A. A., Zhang, J., Zhang, Z., Miller, W. and Lipman, D. J.** (1997). Gapped BLAST and PSI-BLAST: a new generation of protein database search programs. *Nucleic Acids Res.* **25**, 3389-3402.
- Axelrod, J. D., Miller, J. R., Shulman, J. M., Moon, R. T. and Perrimon, N.** (1998). Differential recruitment of Dishevelled provides signaling specificity in the planar cell polarity and Wingless signaling pathways. *Genes Dev.* **12**, 2610-2622.
- Basham, S. E. and Rose, L. S.** (2001). The *Caenorhabditis elegans* polarity gene *ooc-5* encodes a Torsin-related protein of the AAA ATPase superfamily. *Development* **128**, 4645-4656.
- Bateman, A., Birney, E., Durbin, R., Eddy, S. R., Finn, R. D. and Sonnhammer, E. L.** (1999). Pfam 3.1: 1313 multiple alignments and profile HMMs match the majority of proteins. *Nucleic Acids Res.* **27**, 260-262.
- Bowerman, B. and Shelton, C. A.** (1999). Cell polarity in the early *Caenorhabditis elegans* embryo. *Curr. Opin. Genet. Dev.* **9**, 390-395.
- Boyd, L., Levitan, D., Guo, S., Stinchcomb, D. and Kemphues, K. J.** (1996). PAR-2 is asymmetrically distributed and promotes association of P granules and PAR-1 with the cortex in *C. elegans* embryos. *Development* **122**, 3075-3084.
- Brenner, S.** (1974). The genetics of *Caenorhabditis elegans*. *Genetics* **77**, 71-94.
- Cheng, N. N., Kirby, C. and Kemphues, K. J.** (1995). Control of cleavage spindle orientation in *C. elegans*: the role of the *par-2* and *par-3* genes. *Genetics* **139**, 549-555.
- Doe, C. Q. and Bowerman, B.** (2001). Asymmetric cell division: fly neuroblast meets worm zygote. *Curr. Opin. Cell Biol.* **13**, 68-75.
- Etamad-Moghadam, B., Guo, S. and Kemphues, K. J.** (1995). Asymmetrically distributed PAR-3 protein contributes to cell polarity and spindle alignment in early *C. elegans* embryos. *Cell* **83**, 743-752.
- Fire, A., Xu, S., Montgomery, M. K., Kostas, S. A., Driver, S. E. and Mello, C. C.** (1998). Potent and specific genetic interference by double-stranded RNA in *Caenorhabditis elegans*. *Nature* **391**, 806-811.
- Goldstein, B. and Hird, S. N.** (1996). Specification of the anteroposterior axis in *Caenorhabditis elegans*. *Development* **122**, 1467-1474.
- Gönczy, P., Pichler, S., Kirkham, M. and Hyman, A. A.** (1999). Cytoplasmic dynein is required for distinct aspects of MTOC positioning, including centrosome separation, in the one cell stage *Caenorhabditis elegans* embryo. *J. Cell Biol.* **147**, 135-150.
- Gönczy, P., Bellanger, J. M., Kirkham, M., Poznaniowski, A., Baumer, K., Phillips, J. B. and Hyman, A. A.** (2001). *zyg-8*, a gene required for spindle positioning in *C. elegans*, encodes a doublecortin-related kinase that promotes microtubule assembly. *Dev. Cell* **1**, 363-375.
- Gotta, M. and Ahringer, J.** (2001a). Axis determination in *C. elegans*: initiating and transducing polarity. *Curr. Opin. Genet. Dev.* **11**, 367-373.
- Gotta, M. and Ahringer, J.** (2001b). Distinct roles for Galpha and Gbetagamma in regulating spindle position and orientation in *Caenorhabditis elegans* embryos. *Nat. Cell Biol.* **3**, 297-300.
- Grill, S. W., Gönczy, P., Stelzer, E. H. and Hyman, A. A.** (2001). Polarity controls forces governing asymmetric spindle positioning in the *Caenorhabditis elegans* embryo. *Nature* **409**, 630-633.
- Hyman, A. A.** (1989). Centrosome movement in the early divisions of *Caenorhabditis elegans*: a cortical site determining centrosome position. *J. Cell Biol.* **109**, 1185-1194.
- Hyman, A. A. and White, J. G.** (1987). Determination of cell division axes in the early embryogenesis of *Caenorhabditis elegans*. *J. Cell Biol.* **105**, 2123-2135.
- Keating, H. H. and White, J. G.** (1998). Centrosome dynamics in early embryos of *Caenorhabditis elegans*. *J. Cell Sci.* **111**, 3027-3033.
- Kirby, C., Kusch, M. and Kemphues, K.** (1990). Mutations in the *par* genes of *Caenorhabditis elegans* affect cytoplasmic reorganization during the first cell cycle. *Dev. Biol.* **142**, 203-215.
- Knust, E.** (2001). G protein signaling and asymmetric cell division. *Cell* **107**, 125-128.
- Matthews, L. R., Carter, P., Thierry-Mieg, D. and Kemphues, K.** (1998). ZYG-9, a *Caenorhabditis elegans* protein required for microtubule organization and function, is a component of meiotic and mitotic spindle poles. *J. Cell Biol.* **141**, 1159-1168.
- Mello, C. and Fire, A.** (1995). DNA transformation. In *Caenorhabditis elegans. Modern Biological Analysis of an Organism* (ed. H. F. Epstein and D. C. Shakes), pp. 451-482. San Diego: Academic Press.
- Miller, D. M. and Shakes, D. C.** (1995). Immunofluorescence microscopy. In *Caenorhabditis elegans. Modern Biological Analysis of an Organism* (ed. H. F. Epstein and D. C. Shakes), pp. 365-394. San Diego: Academic Press.
- Miller, K. G. and Rand, J. B.** (2000). A role for RIC-8 (Synembryn) and GOA-1 (G(o)alpha) in regulating a subset of centrosome movements during early embryogenesis in *Caenorhabditis elegans*. *Genetics* **156**, 1649-1660.
- Ponting, C. P. and Bork, P.** (1996). Pleckstrin's repeat performance: a novel domain in G-protein signaling? *Trends Biochem. Sci.* **21**, 245-246.
- Rose, L. S. and Kemphues, K.** (1998a). The *let-99* gene is required for proper spindle orientation during cleavage of the *C. elegans* embryo. *Development* **125**, 1337-1346.
- Rose, L. S. and Kemphues, K. J.** (1998b). Early patterning of the *C. elegans* embryo. *Annu. Rev. Genet.* **32**, 521-545.

- Salmon, E. D.** (1989). Cytokinesis in animal cells. *Curr. Opin. Cell Biol.* **1**, 541-547.
- Schierenberg, E.** (1987). Reversal of cellular polarity and early cell-cell interaction in the embryo of *Caenorhabditis elegans*. *Dev. Biol.* **122**, 452-463.
- Schubert, C. M., Lin, R., de Vries, C. J., Plasterk, R. H. and Priess, J. R.** (2000). MEX-5 and MEX-6 function to establish soma/germline asymmetry in early *C. elegans* embryos. *Mol. Cell* **5**, 671-682.
- Schultz, J., Copley, R. R., Doerks, T., Ponting, C. P. and Bork, P.** (2000). SMART: a web-based tool for the study of genetically mobile domains. *Nucleic Acids Res.* **28**, 231-234.
- Skop, A. R. and White, J. G.** (1998). The dynactin complex is required for cleavage plane specification in early *Caenorhabditis elegans* embryos. *Curr. Biol.* **8**, 1110-1116.
- Stein, L., Sternberg, P., Durbin, R., Thierry-Mieg, J. and Spieth, J.** (2001). WormBase: network access to the genome and biology of *Caenorhabditis elegans*. *Nucleic Acids Res.* **29**, 82-86.
- The *C. elegans* Sequencing Consortium** (1998). Genome sequence of the nematode *C. elegans*: a platform for investigating biology. *Science* **282**, 2012-2018.
- Waddle, J. A., Cooper, J. A. and Waterston, R. H.** (1994). Transient localized accumulation of actin in *Caenorhabditis elegans* blastomeres with oriented asymmetric divisions. *Development* **120**, 2317-2328.
- Wallenfang, M. R. and Seydoux, G.** (2000). Polarization of the anterior-posterior axis of *C. elegans* is a microtubule-directed process. *Nature* **408**, 89-92.
- Watts, J. L., Morton, D. G., Bestman, J. and Kemphues, K. J.** (2000). The *C. elegans par-4* gene encodes a putative serine-threonine kinase required for establishing embryonic asymmetry. *Development* **127**, 1467-1475.
- Wolf, N., Priess, J. and Hirsh, D.** (1983). Segregation of germline granules in early embryos of *Caenorhabditis elegans*: an electron microscopic analysis. *J. Embryol. Exp. Morphol.* **73**, 297-306.
- Wong, H. C., Mao, J., Nguyen, J. T., Srinivas, S., Zhang, W., Liu, B., Li, L., Wu, D. and Zheng, J.** (2000). Structural basis of the recognition of the dishevelled DEP domain in the Wnt signaling pathway. *Nat. Struct. Biol.* **7**, 1178-1184.
- Zwaal, R. R., Ahringer, J., van Luenen, H. G. A. M., Rushforth, A., Anderson, P. and Plasterk, R. H. A.** (1996). G proteins are required for spatial orientation of early cell cleavages in *C. elegans* embryos. *Cell* **86**, 619-629.